Electronic Supplementary Material (ESI) for Analyst

Supporting Information

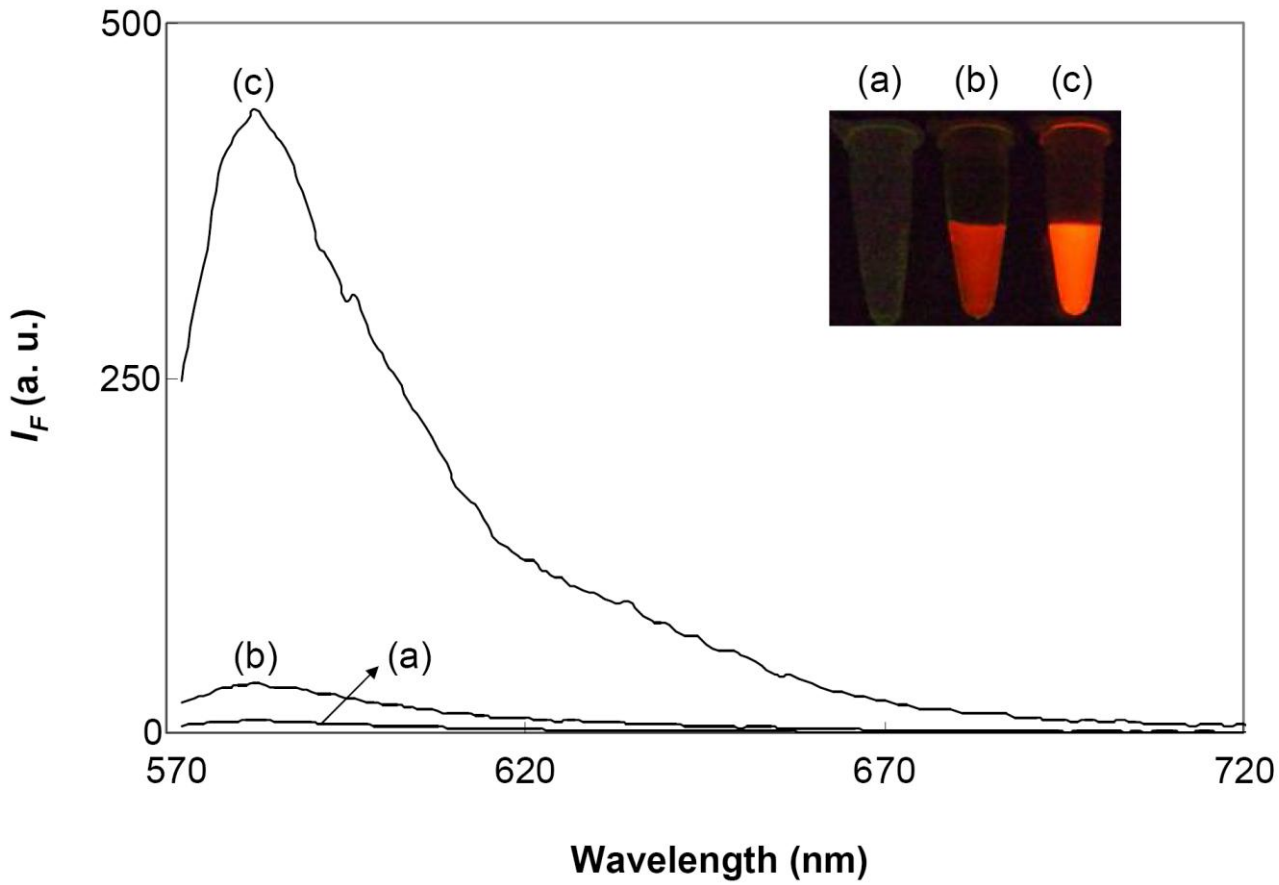

Fig. S1. Fluorescence spectra of Tris-acetate solutions (5 mM, pH 8.0) containing AUR (10 μM), H_2O_2 (0.4 mM) and (a) T30695 (100 nM), (b) citrate-capped Au NPs (0.3 nM), or (c) 40T30695–Au NPs (0.3 nM) in the presence of Pb^{2+} ions (100 nM). Inset: Photograph of the fluorescence of the solutions upon excitation under a hand-held UV lamp (365 nm). Other conditions were the same as those described in Figure 1.

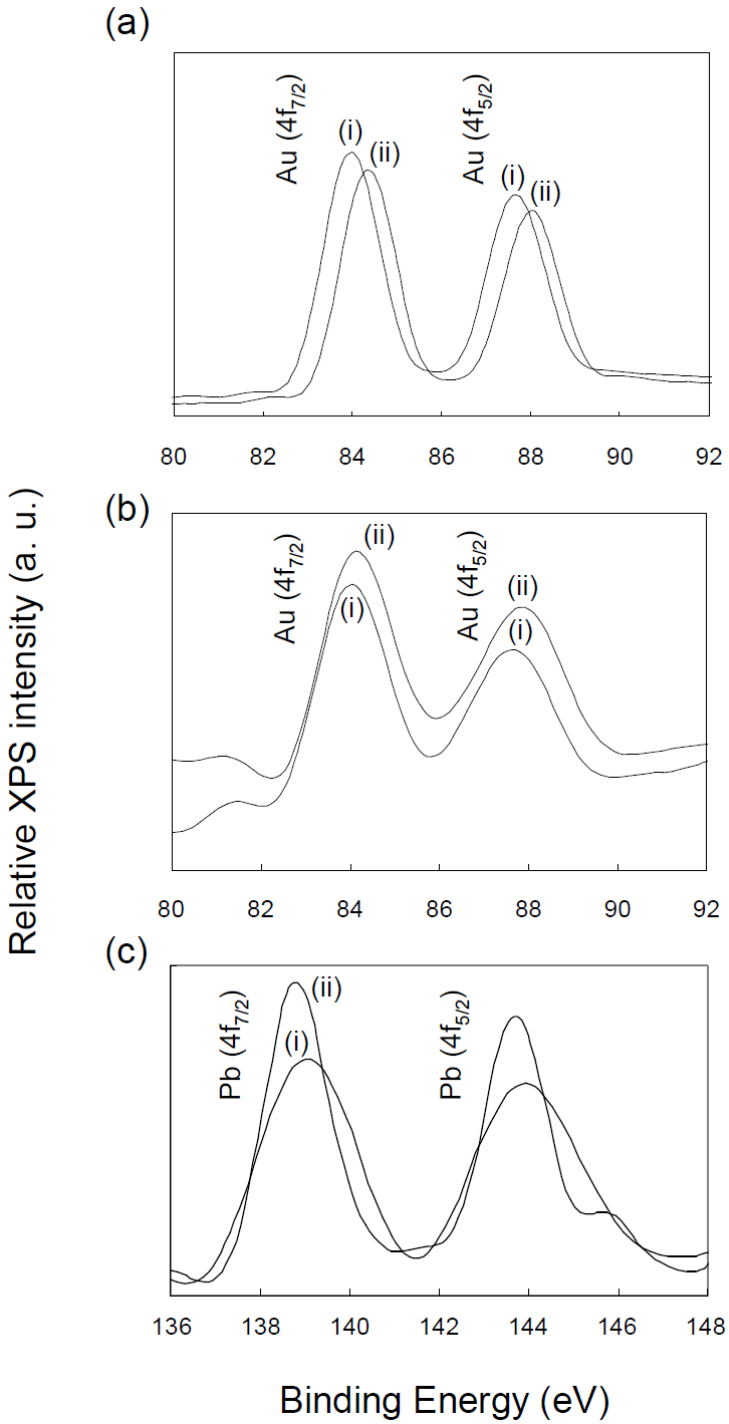

Fig. S2. XPS spectra of the (a) citrate-capped Au NPs (14.9 nM, 30 μL) and (b) 40T30695–Au NPs (14.9 nM, 30 μL) reveals the signals for the Au $4f_{7/2}$ electrons in the (i) absence and (ii) presence of Pb^{2+} ions (1 μM) respectively. As well as for the (c) Pb $4f_{7/2}$ electrons in the presence of Pb^{2+} ions (1 μM) of (i) citrate-capped Au NPs and (ii) 40T30695–Au NPs respectively.

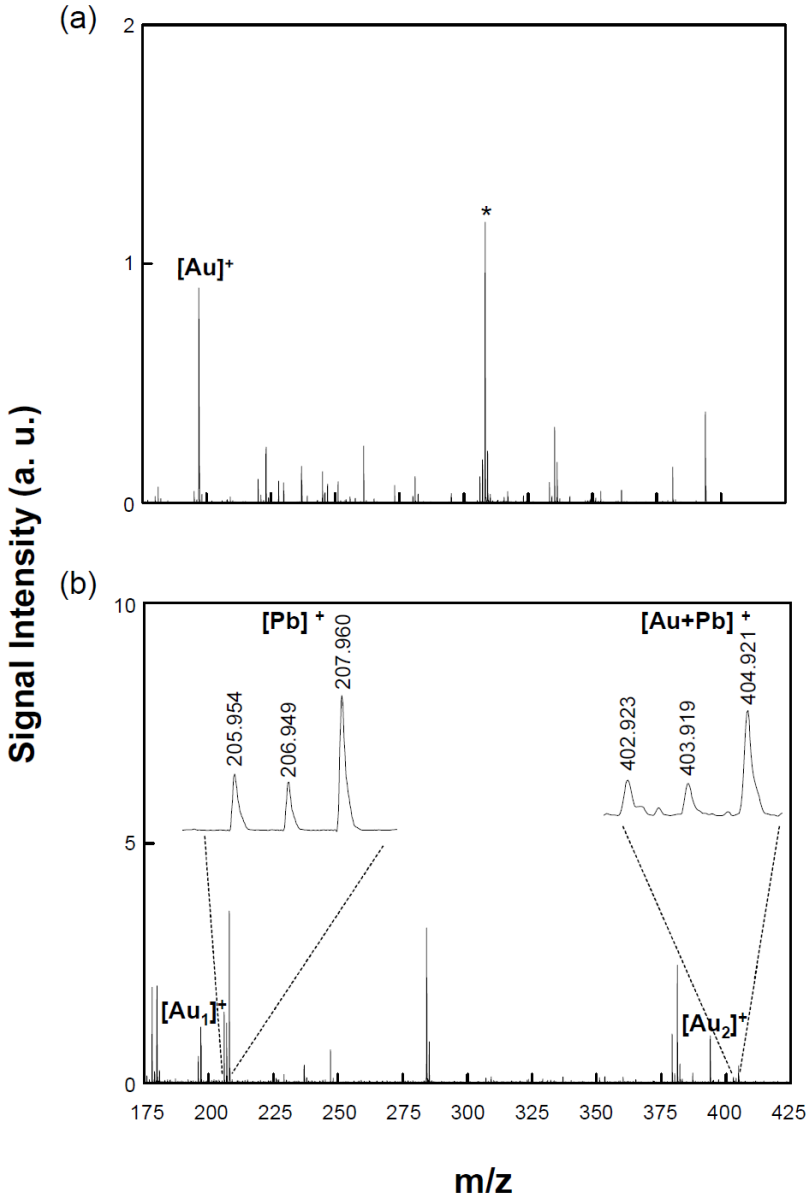

Fig. S3. SALDI mass spectra of solutions containing Tris-acetate buffers (5 mM, pH 8.0), (a) 40T30695–Au NPs (7.5 nM) in the absence of Pb^{2+} ions, and (b) citrate-capped Au NPs (7.5 nM) in the presence of Pb^{2+} ions (10 μM).The asterisk (*) represent unknown peaks. (a) The peak at *m*/*z* 196.94 is assigned to $[Au]^+$ ions, (b) The peak at *m*/*z* 196.96, 393.93, (205.95, 206.95, 207.96) and (402.92, 403.92, 404.92) are assigned to $[Au_1]^+$, $[Au_2]^+$, $[Pb]^+$ and $[Au+Pb]^+$ ions, respectively. In total, 300 pulsed laser shots were applied under a laser fluence of 62.5 μJ. Other conditions were the same as those described in Figure 2.

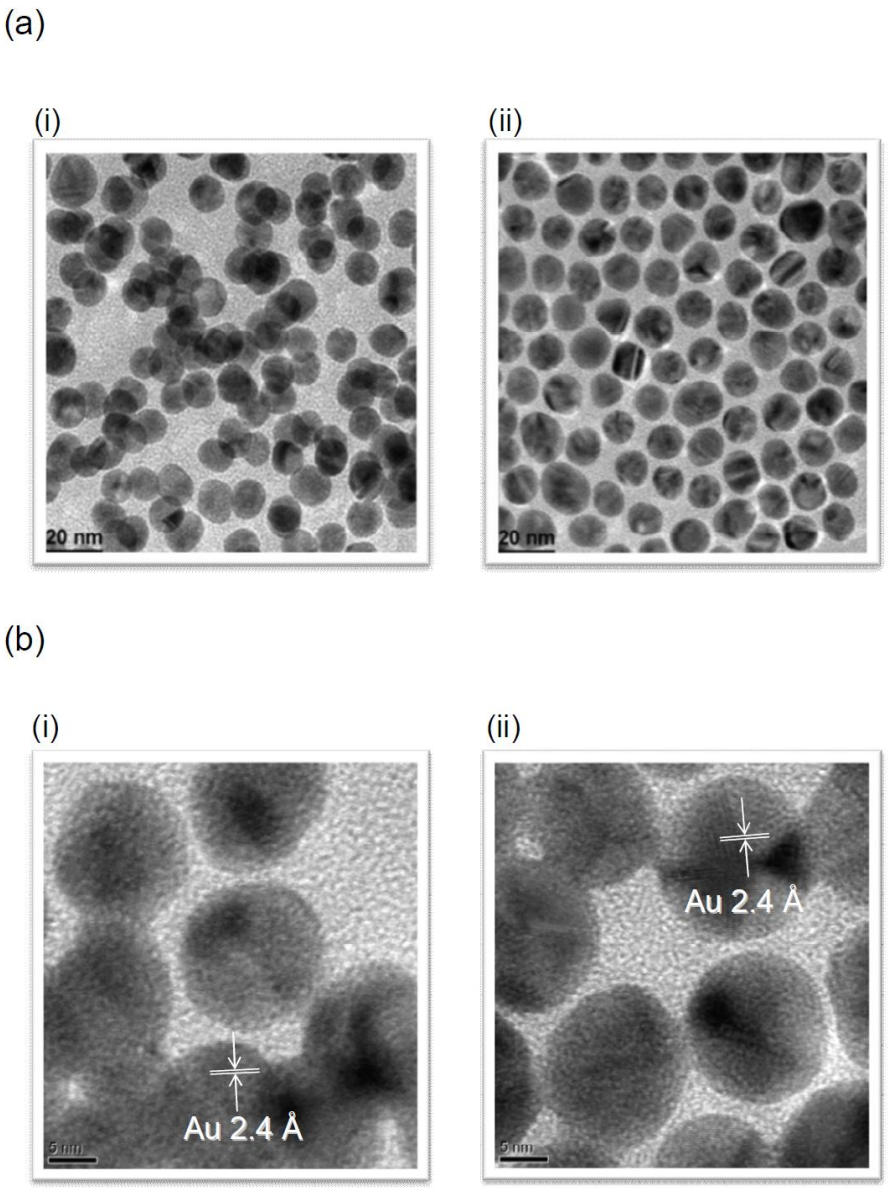

Fig. S4. (a) Transmission electron microscopy (TEM) and (b) high resolution transmission electron microscopy (HRTEM) images of 40T30695–Au NPs (0.3 nM) in the (i) absence and (ii) presence of Pb^{2+} ions (10 μM). Other conditions were the same as those described in Figure 1. Average Au NP sizes in Figure S4a(i) and S4a(ii) are 13.6 ± 0.3 and 13.6 ± 0.5 nm, respectively. The lattice fringes in both (a) and (b) are consistent with metallic gold having a discerned lattice spacing of 2.4 Å, which corresponds to the d-spacing of the (111) crystal plane of face-centered cubic (fcc) Au.

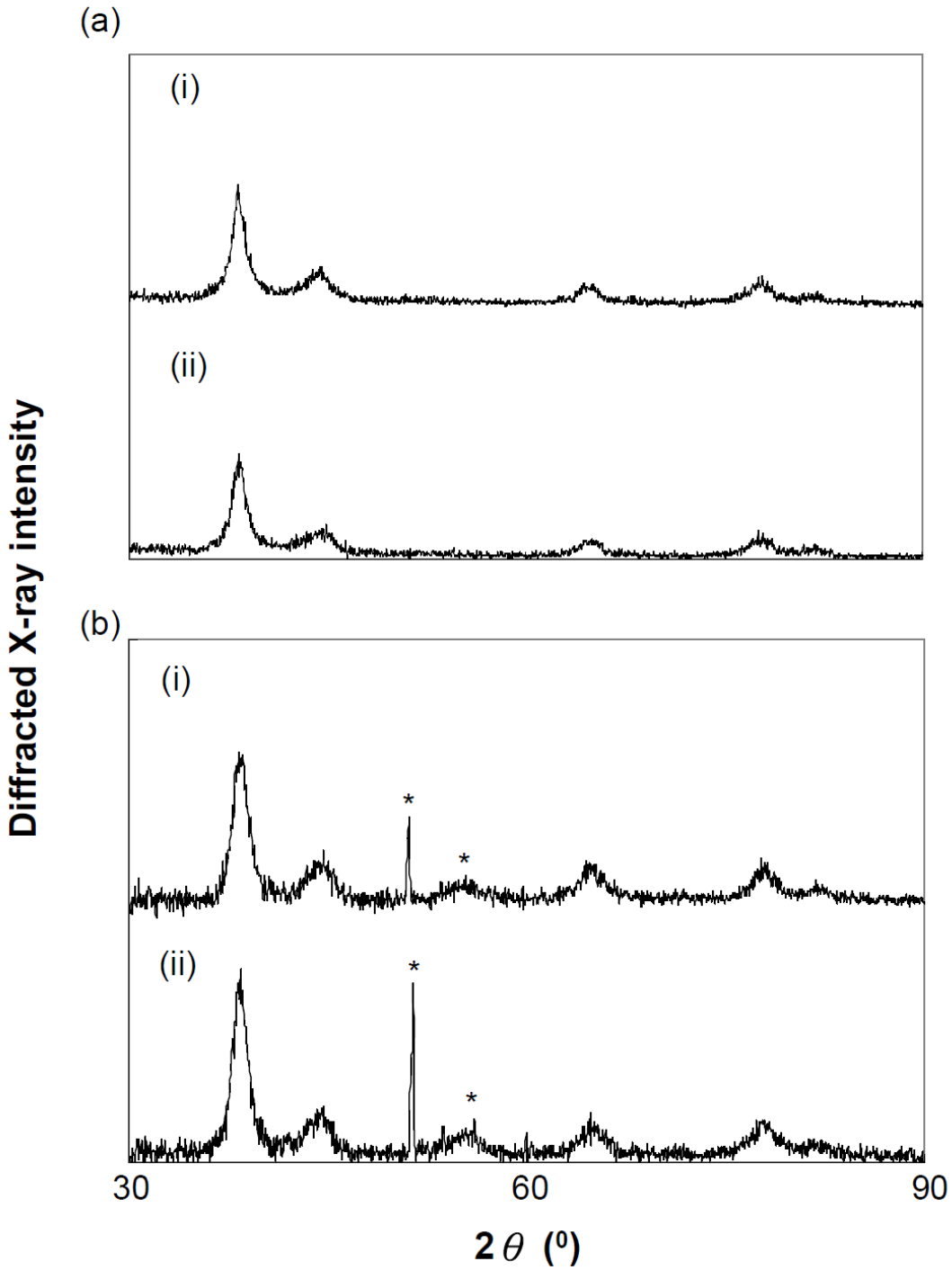

Fig. S5. XRD patterns of (a) citrate-capped Au NPs (60 nM) and (b) 40T30695–Au NPs (60 nM) in the (i) absence and (ii) presence of Pb^{2+} ions (10 μM), respectively. The asterisk (*) represent unknown peaks.

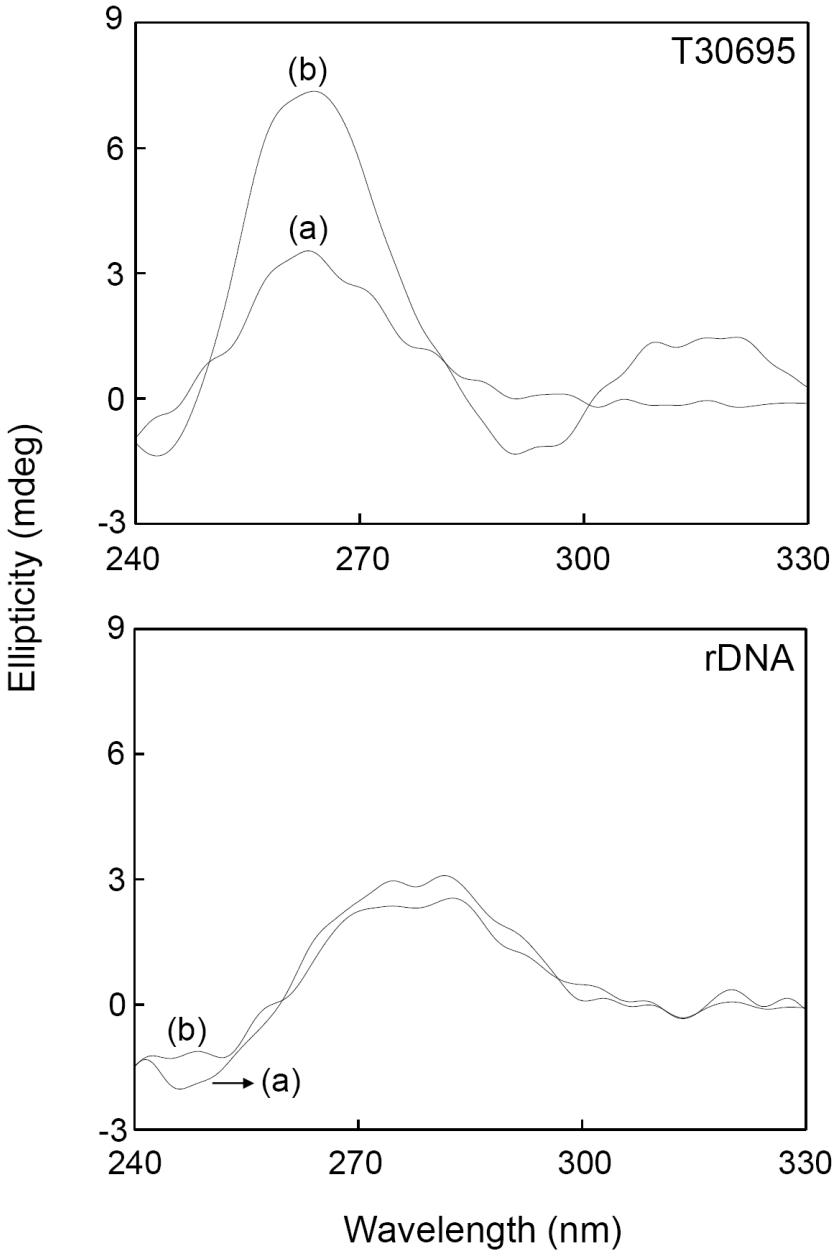

Fig. S6. Circular dichroism (CD) spectra of T30695 and random DNA (rDNA) oligonucleotides (1.0 μM) in the (a) absence and (b) presence of Pb^{2+} (10 μM) ions. Solutions were prepared in 5 mM Tris-acetate (pH 8.0).

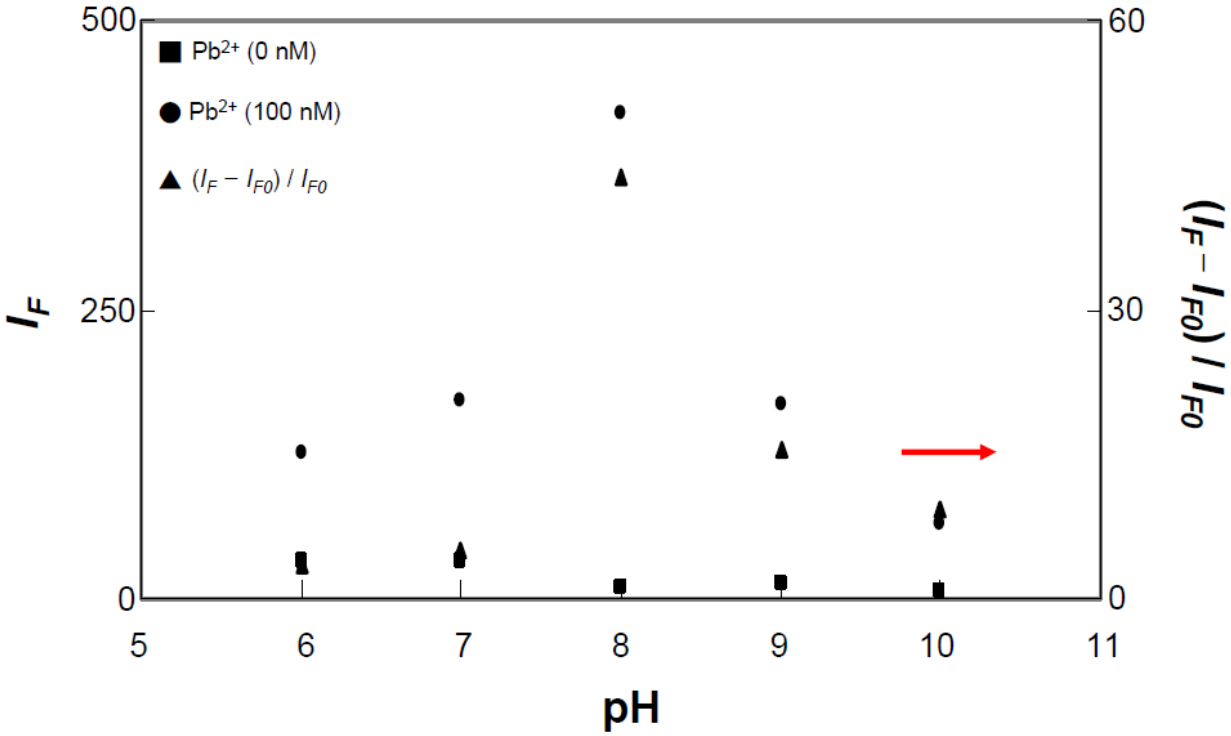

Fig. S7. Effect of pH (6.0–10.0) on the fluorescence intensity of the 40T30695–Au NP/AUR probe (0.3 nM) in 5 mM Tris-acetate buffer in the absence and presence of Pb^{2+} ions (100 nM). Other conditions were the same as those described in Figure 1. I_{F0} and I_F are the fluorescence intensities of the solutions in the absence and presence of Pb^{2+} ions, respectively.

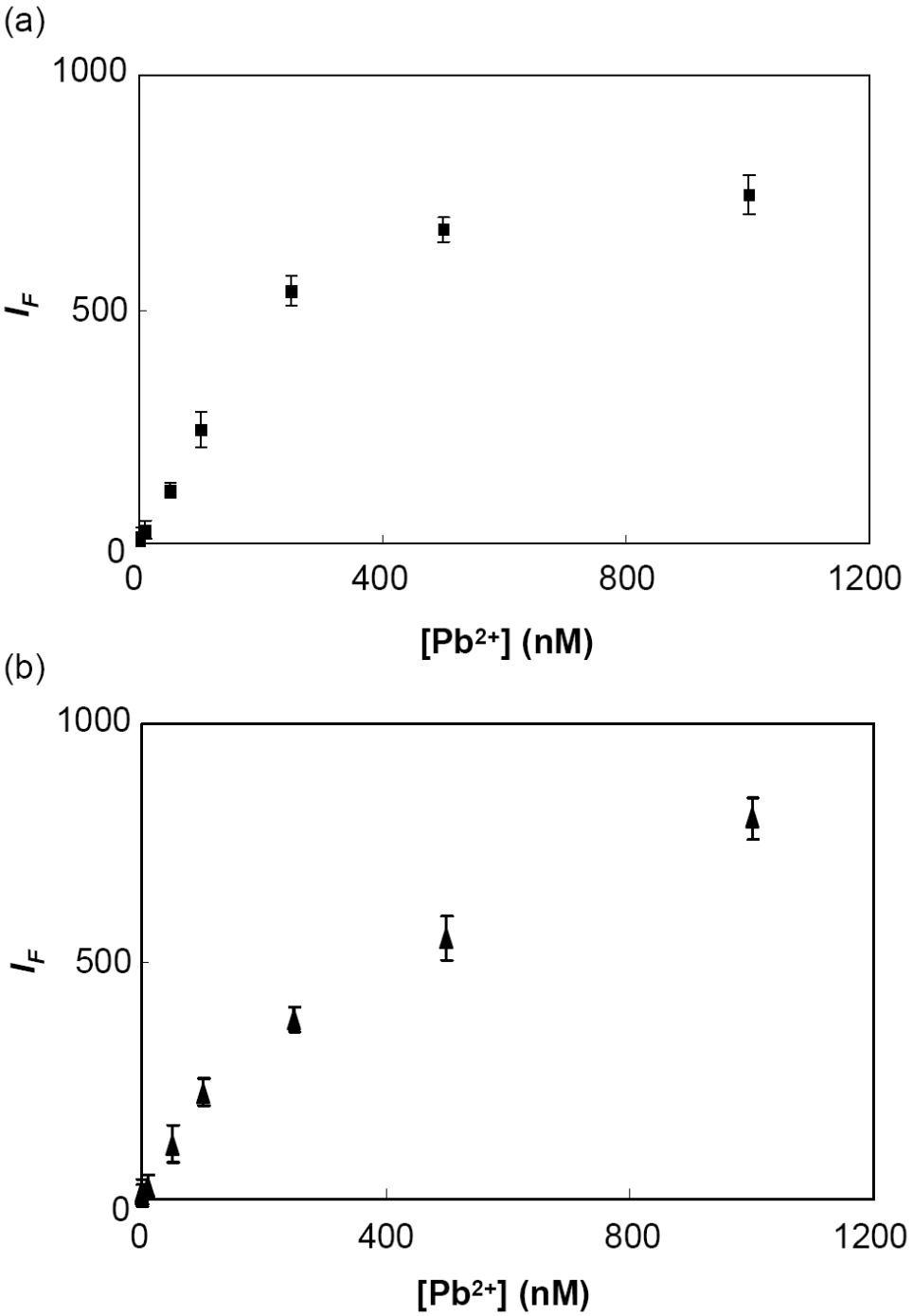

Fig. S8. Validation of the 40T30695–Au NP/AUR probe for the sensing of Pb^{2+} ions (0–1 μM) in 5 mM Tris-acetate solutions (pH 8.0) containing (a) 150 mM NaCl, 5 mM KCl, 1 mM $MgCl_2$, and 1 mM $CaCl_2$ or (b) 10 μM cysteine. Other conditions were the same as those described in Figure 1.

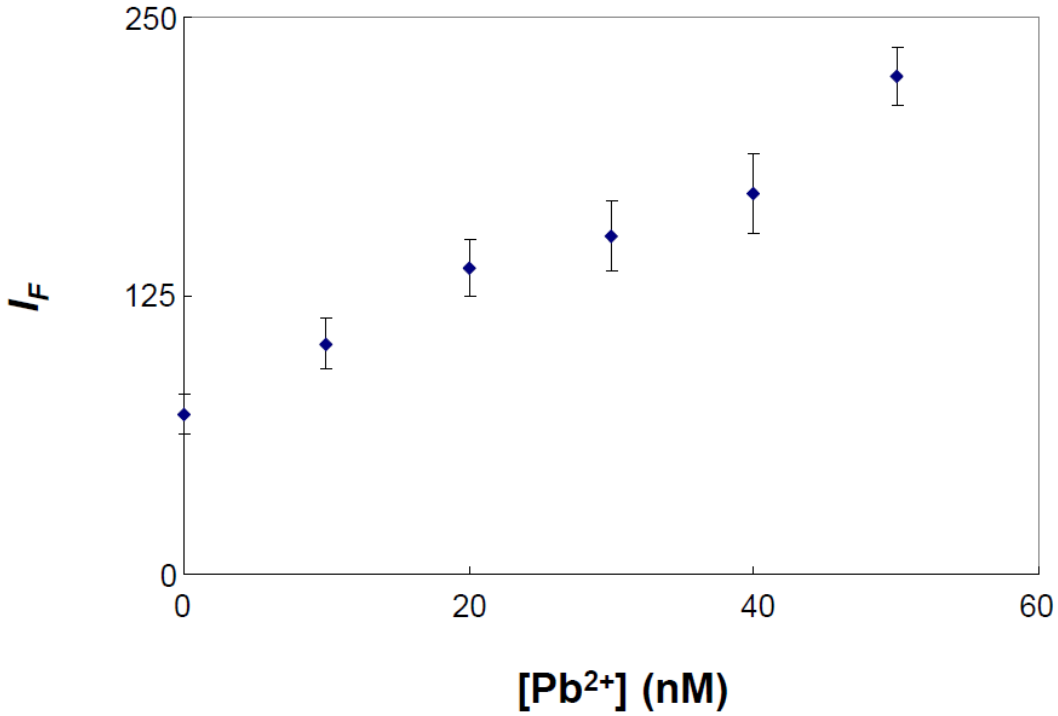

Fig. S9. Blood sample analysis of a healthy adult male (25 years old) using the 40T30695–Au NP/AUR probe. Aliquots of the diluted (3-fold) blood sample were spiked with Pb^{2+} ions at concentrations between 0–50 nM. Other conditions remains the same as those described in Figure 1.

5